

Chapter 6

Quantifying Human-Humanoid Imitation Activities

6.1 Introduction

Similarly as in Chapter 5, in this Chapter, results for experiments of human-humanoid imitation activities, described in Section 4.5.2, are presented by including time series, minimum embedding parameters, the reconstructed state spaces (RSS) using uniform time-delay embedding technique (UTDE), recurrence plots (RP), recurrent quantification analysis (RQA), and weaknesses and strengthens of RQA with three dimensional surface plots of RQA.

Time series data for this experiment are described as follows:

- Twenty participants defined as pN where N is the number of participant.
- Three levels of smoothness for the normalised data (sg0zmuv, sg1zmuv and sg2zmuv), computed from two different filter lengths (29 and 159) with the same polynomial degree of 5 using the function `sgolay(p,n,m)` (signal R developers, 2014),

Quantifying Human-Humanoid Imitation Activities

- Four window length size: 2-sec (100 samples), 5-sec (250 samples), 10-sec (500 samples) and 15-sec (750 samples), and
- Four velocities of arm movement activity: horizontal normal (HN), horizontal faster (HF), vertical normal (VN) and vertical faster (VF)

To make the visual comparison easier, time series for only three participants (*p01*, *p02*, *p03*) with a window length of 10 seconds (500 samples) are considered for the following results. See Appendix F for further results.

6.2 Time series

Figures 6.1 and 6.2 show time series of horizontal arm movements using axis GyroZ and vertical arm movements using axis GyroY. The remaining time series are presented in Appendix F.1.

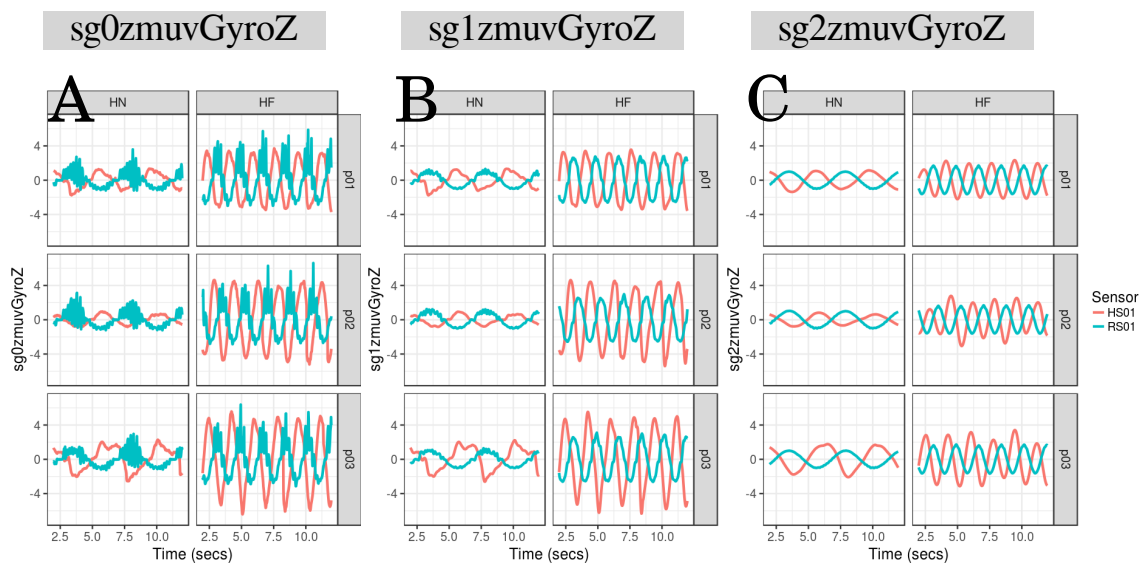


Fig. 6.1 Time series for horizontal arm movements. (A) raw-normalised (sg0zmuvGyroZ), (B) normalised-smoothed 1 (sg1zmuvGyroZ) and (C) normalised-smoothed 2 (sg2zmuvGyroZ). Time series are only for three participants ($p01$, $p02$, and $p03$) for horizontal movements in normal and faster velocity (HN, HF) with the normalised GyroZ axis (zmuvGyroZ) and with one sensor attached to the participant (HS01) and other sensor attached to the robot (RS01). R code to reproduce the figure is available at [🔗](#).

Quantifying Human-Humanoid Imitation Activities

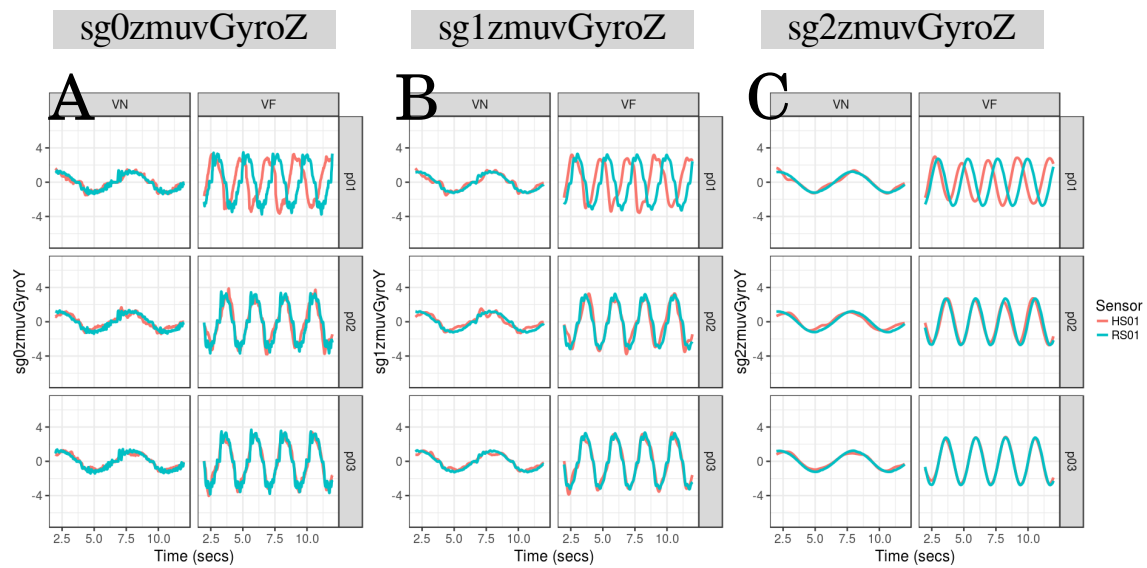


Fig. 6.2 Time series for vertical arm movements. (A) raw-normalised ($sg0zmuvGyroY$), (B) normalised-smoothed 1 ($sg1zmuvGyroY$) and (C) normalised-smoothed 2 ($sg2zmuvGyroY$). Time series are only for three participants ($p01$, $p02$, and $p03$) for vertical movements in normal and faster velocity (VN, VF) with the normalised GyroY axis ($zmuvGyroY$) and with one sensor attached to the participant (HS01) and other sensor attached to the robot (RS01). R code to reproduce the figure is available at [\[link\]](#).

6.3 Minimum Embedding Parameters

As mentioned in Section 5.3 in Chapter 5, minimum embedding parameters using FNN and AMI algorithms are computed for time series of this section. Hence, Figs 6.3(A) show box plots of the minimum embedding dimensions of twenty participants performing horizontal and vertical arm movements at normal and faster velocities (HN, HF, VN and VF) with attached sensors to participants (HS01) and to the robot (RS01). Generally, Figs 6.3(A) show that minimum embedding values appear to be constant for sensor RS01 as their interquartile range in the box plots are near to 0.1 with the exception of two axis. Minimum embedding values for sensor HS01 appear to show more variations as their interquartile range of the box plots are near to 1 with four exceptions. Additionally, it can be seen in Figs 6.3(A) that there is a decrease of mean values (rhombus) in the box plots as smoothness of time series increase. See Figs. F.7 and F.8 in Appendix F.2 for detailed values of embedding dimensions for each participant.

Similarly, the first minimum values of AMI values for participants ($p01$ to $p20$), activities (HN, HF, VN, and VF) and sensors (HS01, RS01) are shown in the box plots of Figs 6.3(B). It can be seen that values for HS01 tend to be more spread as the smoothness of the time series is increasing (see the increase of both mean (rhombus) and interquartile range). However, AMI values for RS01 do not show such a similar increase in relation with the increase of smoothness excepting for HF and VF (see the increase of both mean (rhombus) and interquartile range) (Figs 6.3(B)). Similarly to the minimum parameters in Chapter 5 (see 5.3), there is a decrease of minimum embedding dimension as the smoothness is increasing, meaning that there is a decrease of the dynamics of the time series data. Also, the sample mean (gray rhombus) of first minimum AMI increase as the smoothness increase, meaning that the maximal

Quantifying Human-Humanoid Imitation Activities

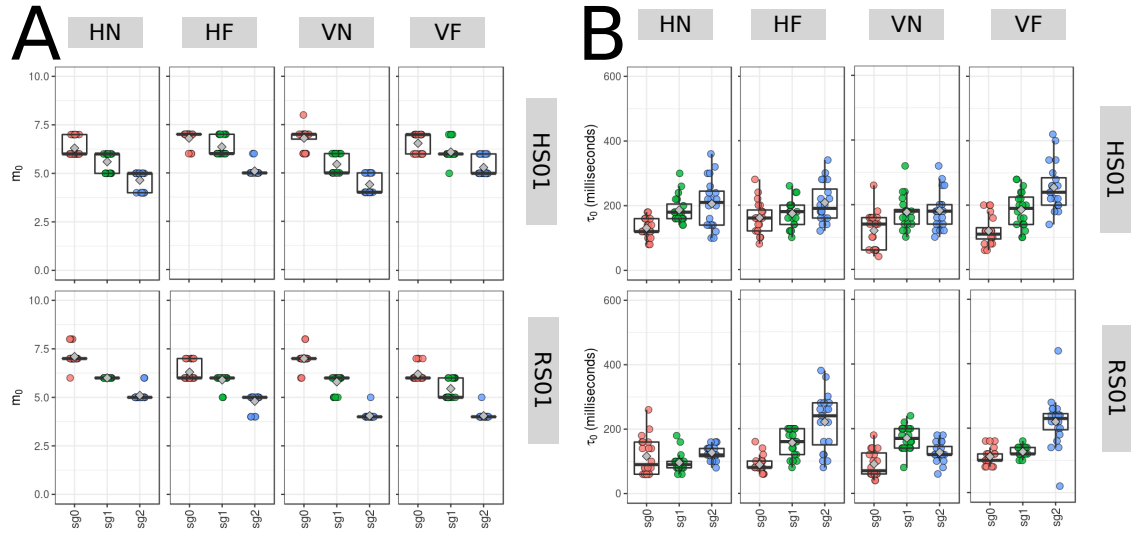


Fig. 6.3 Box plots of minimum embedding parameters. Box plots of (A) minimum embedding dimensions and (B) first minimum AMI values for Horizontal Normal (HN), Horizontal Faster (HF), Vertical Normal (VN) and Vertical Faster (VF) with sensors attached to participants (HS01) and sensor attached to robot (RS01). Minimum embedding dimensions (m_0 and τ_0) are for twenty participants ($p01$ to $p20$) with three smoothed signals (sg0zmuvGyroZ (sg0) , sg1zmuvGyroZ (sg1) and sg2zmuvGyroZ (sg2)) and window length of 10-sec (500 samples). R code to reproduce the figure is available at [\(R\)](#).

information to knowledge at τ_0 also increase. See Figs. F.9 and F.10 in Appendix F.2 for more details about AMI values for each participant.

6.3.1 Average minimum embedding parameters

Following the Section 3.4.3 to compute the overall average of minimum embedding parameters, the sample mean for the minimum values of $E_1(m)$ from Figs 6.3(A) is $\bar{m}_0 = 6$ and the sample mean for minimum values of AMIs from Figs 6.3(B) is $\bar{\tau}_0 = 8$, for which the overall average minimum embedding parameters is ($\bar{m}_0 = 6$, $\bar{\tau}_0 = 8$). Hence, the average minimum embedding parameters ($\bar{m}_0 = 6$, $\bar{\tau}_0 = 8$) has been considered to compute Reconstructed State Spaces (RSSs), Recurrence Plots (RPs) and Recurrence Quantification Analysis (RQA) metrics for human-humanoid activities.

6.4 Reconstructed state spaces with UTDE

Considering Section 3.5 and time series for participant *p01* (Figs 6.1, 6.2) the reconstructed state spaces for horizontal arm movements (Figs 6.4) and vertical arm movements (Figs 6.5) are computed with $\bar{m}_0 = 6$ and $\bar{\tau}_0 = 8$

The trajectories of the RSSs for horizontal normal and faster from HS01 and RS01 are slightly smoothed as the time-series smoothness increase (Figs 6.4). Although the frequency of the movement increase from normal to faster velocity activities, the trajectories RSSs in Figs 6.4(B) show higher oscillations specially for a maximum values of smoothness (sg2zmuvGyroZ), while the trajectories in the RSS for HF in Figs 6.4(D) show a lower and smoothed oscillations as the smoothness increase. In contrast, the time series for vertical movements are less noisy and well structured (Figs 6.2) for which the trajectories in the RSSs seem to be less organised, specially for Fig 6.5(A,C), while time series for vertical faster movements (VF) which have more periods (Figs 6.2) present trajectories in the RSS with well defined patterns (6.5(C,D)). It is important to note that the smoothness of time series also create an effect on

Quantifying Human-Humanoid Imitation Activities

smoothness in the trajectories of the RSS, being the RS01 more organised and more persistent while trajectories for HS01 are more changeable (Figs. 6.4, 6.5).

Therefore, one can observe by eye the differences in each of the trajectories in the reconstructed state spaces (Figs 6.4, 6.5), however one might be not objective when quantifying those differences since such observations might vary from person to person. With that in mind, in early experiments of this thesis, it had been tried to objectively quantify those differences using euclidean distances between the origin to each of the points in the trajectories in the trajectories of the RSSs, however these created suspicious metrics, specially for trajectories which looked very messy. Hence, it has been proposed the application of Recurrence Quantification Analyses (RQA) in order to have a more objective quantification of the differences in each of the cases of the time series.

6.4 Reconstructed state spaces with UTDE

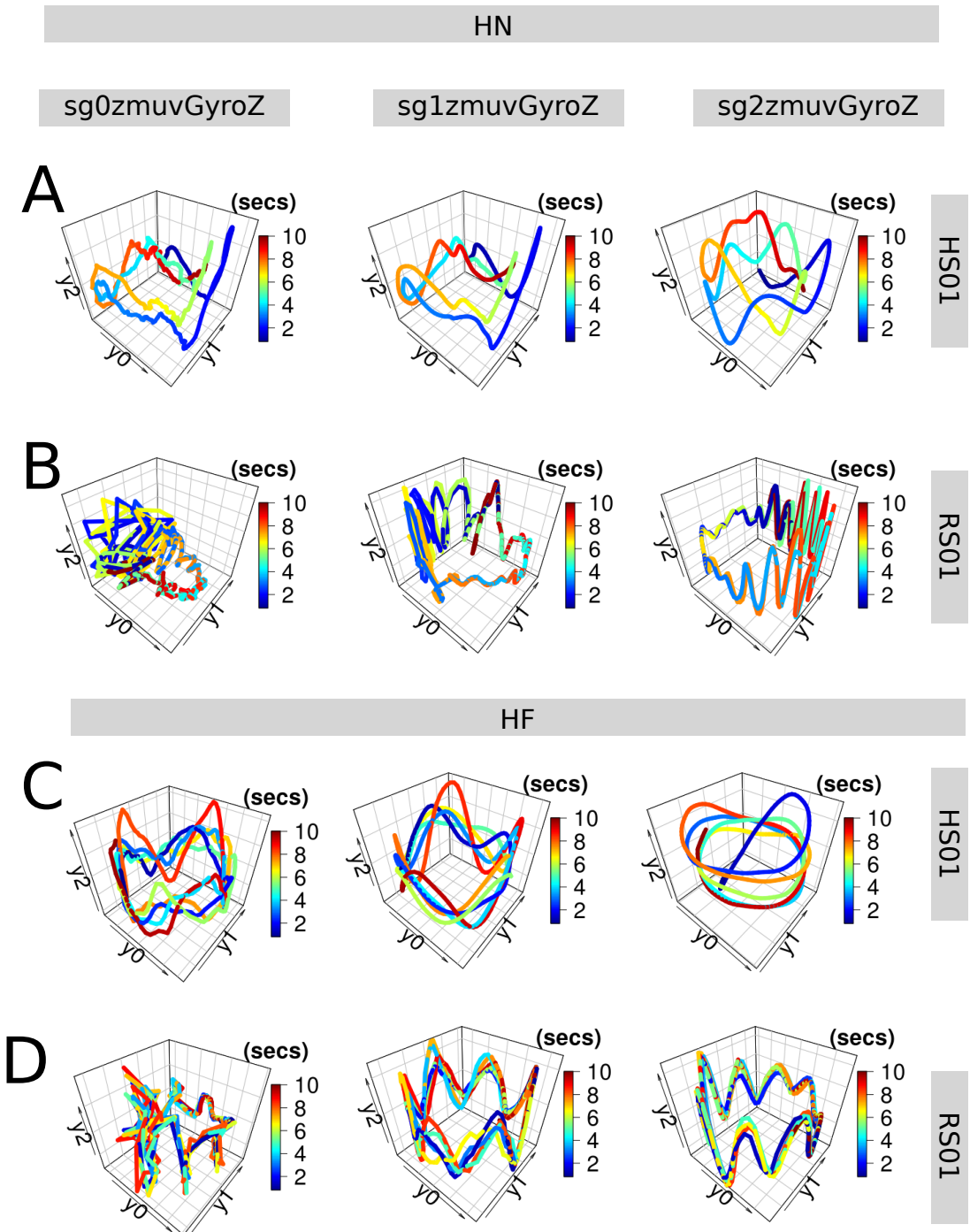


Fig. 6.4 RSSs for horizontal arm movements. Reconstructed state spaces of participant p01 for horizontal movements in normal and faster velocity (HN, HF) with raw-normalised ($sg0zmuvGyroZ$), normalised-smoothed 1 ($sg1zmuvGyroZ$) and normalised-smoothed 2 ($sg2zmuvGyroZ$) time series of the sensors attached to the participant (HS01) and other sensor attached to the robot (RS01). Reconstructed state spaces were computed with embedding parameters $\overline{m}_0 = 6$, $\overline{\tau}_0 = 8$. R code to reproduce the figure is available at [\[link\]](#).

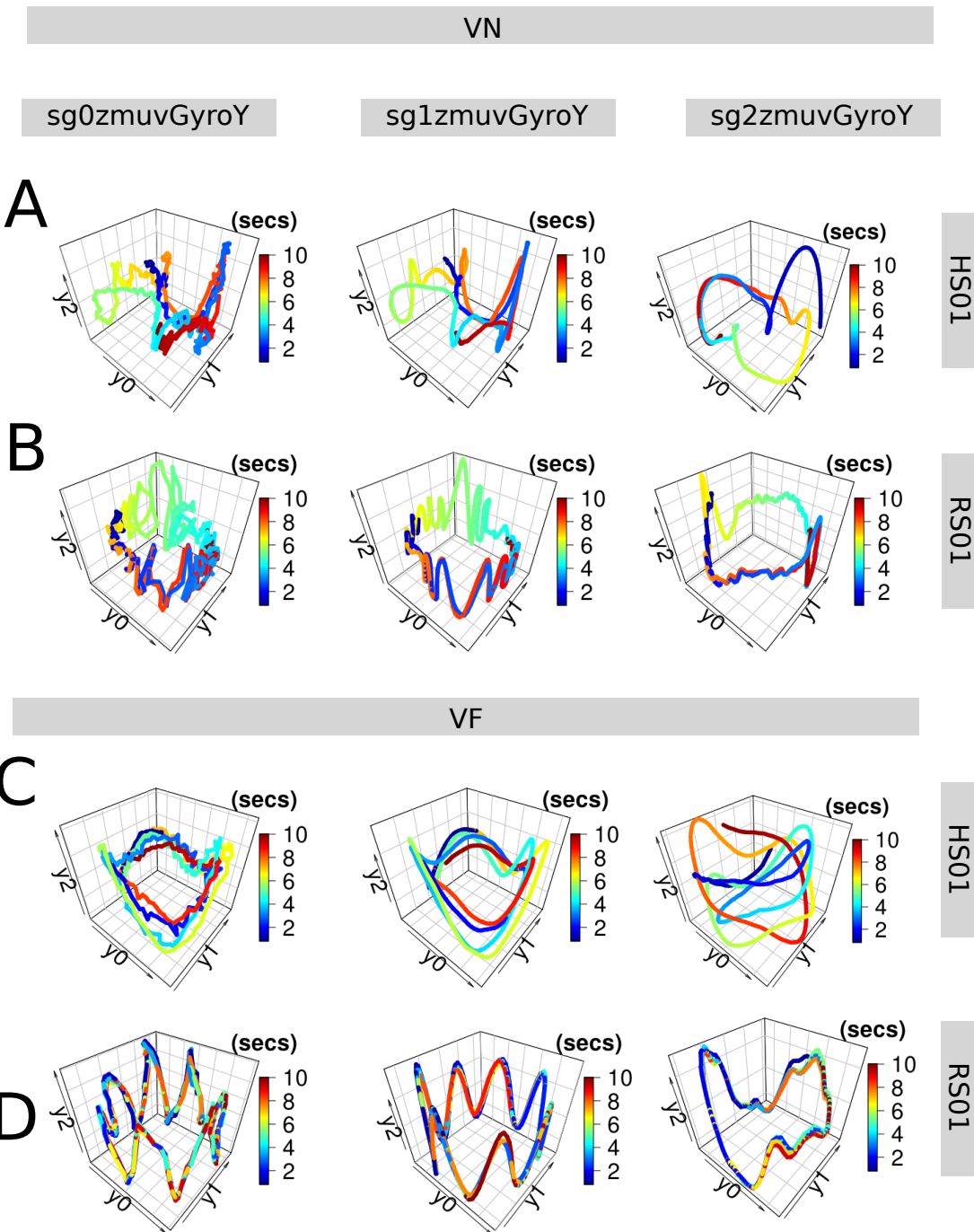


Fig. 6.5 RSSs for vertical arm movements. Reconstructed state spaces of participant p01 for vertical movements in normal and faster velocity (VN, VF) with raw-normalised ($sg0zmuvGyroZ$), normalised-smoothed 1 ($sg1zmuvGyroZ$) and normalised-smoothed 2 ($sg2zmuvGyroZ$) time series of the sensors attached to the participant (HS01) and other sensor attached to the robot (RS01). Reconstructed state spaces were computed with embedding parameters $\overline{m}_0 = 6$, $\overline{\tau}_0 = 8$. R code to reproduce the figure is available at [\[link\]](#).

6.5 Recurrences Plots

Considering the time series of Figs 6.1 and 6.2, Recurrence Plots are computed for horizontal arm movements (Fig 6.6) and vertical arm movements (Fig 6.7) using the average embedding parameters ($\bar{m}_0 = 6$, $\bar{\tau}_0 = 8$) and a recurrence threshold of $\epsilon = 1$. For the selection of the recurrence threshold, Marwan (2011) pointed out that choosing an appropriate recurrence threshold is crucial to get meaningful representations in the RPs, however, for this thesis where quantifying movement variability is our aim, little importance has been given to the selection of the recurrence threshold for the RPs as long as it is able to represent the dynamical transitions in each of the time series.

In general, the increase of smoothness in time series results in thicker and better defined diagonal lines in the RPs (Figs 6.6, 6.7). Additionally, due to the changes in velocities of the movements the patterns in the RPs present an increase of diagonal lines and a decrease of line thickness. Although, the patterns of RPs show consistency with the movements type and velocities changes, it can be noticed that patterns of the RPs for HS01 are not well defined while patterns of the RPs for RS01 shown a more consistent pattern (Fig 6.6, 6.7).

It is important to note that only RPs for participant 01 are presented in (Fig 6.7, 6.6), however other RPs for all participants are presented in Appendix F.4. With that in mind, it can be highlighted that, as similar as, the Reconstructed State Spaces (Figs 6.4, 6.5), the patterns in the RPs can be easily noticed by eye for different conditions of the time series (Figs 6.6, Fig 6.7), however these characteristics in the patterns of the RPs are subjective for the person who analysed them and might vary from person to person. That lead us to apply Recurrence Quantification Analysis (RQA) in order to have an objective quantification metric for the movement variability for each of the conditions of the time series.

Quantifying Human-Humanoid Imitation Activities

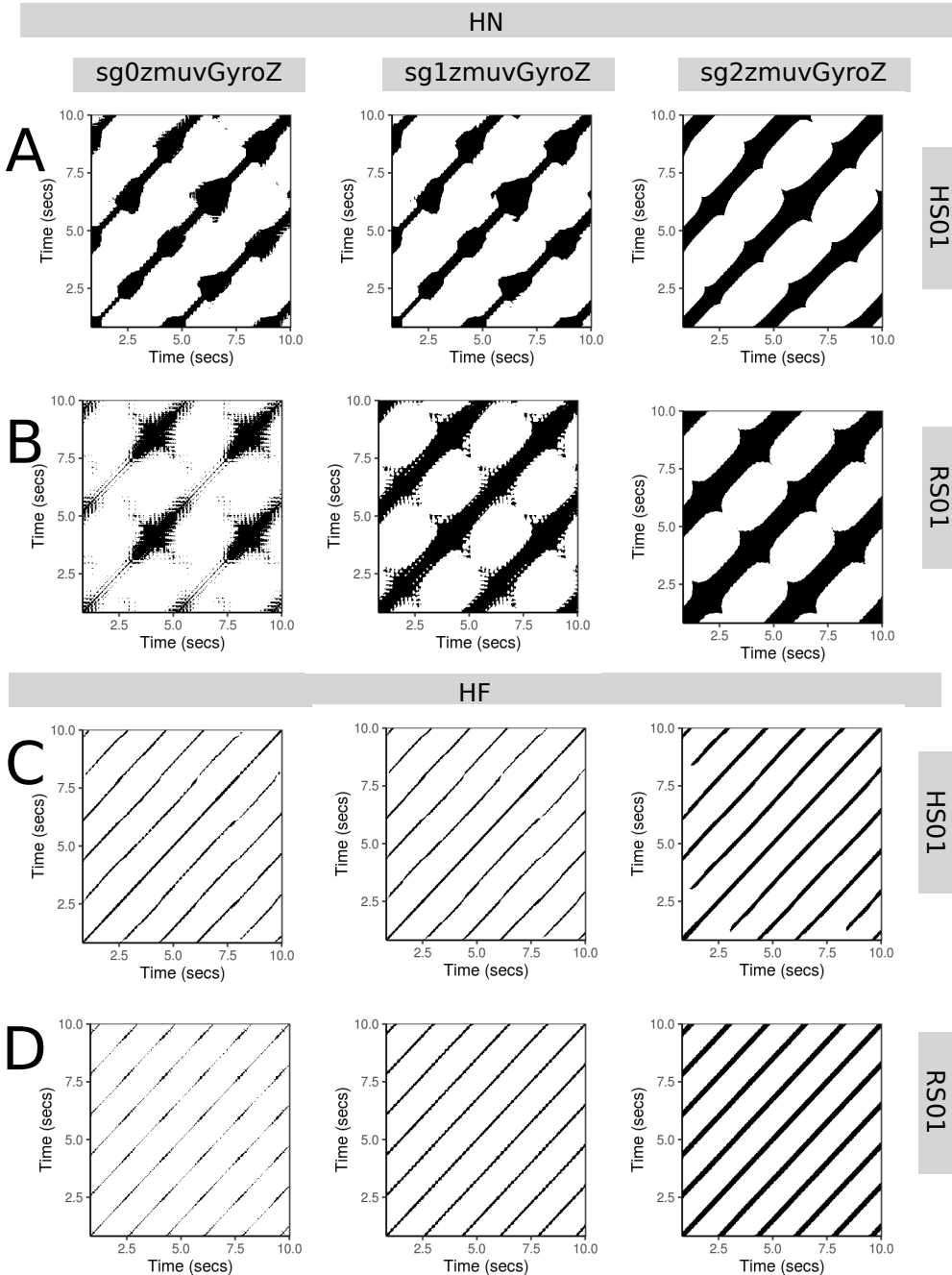


Fig. 6.6 RPs for horizontal arm movements. Recurrence plots of participant $p01$ for horizontal movements in normal and faster velocity (HN, HF) with time series of raw-normalised ($sg0zmuvGyroZ$), normalised-smoothed 1 ($sg1zmuvGyroZ$) and normalised-smoothed 2 ($sg2zmuvGyroZ$), and sensors attached to the participant (HS01) and to the robot (RS01). Recurrence plots were computed with embedding parameters $\overline{m}_0 = 6$, $\overline{\tau}_0 = 8$ and recurrence threshold $\epsilon = 1$. R code to reproduce the figure is available at [DOI](#).

6.5 Recurrences Plots

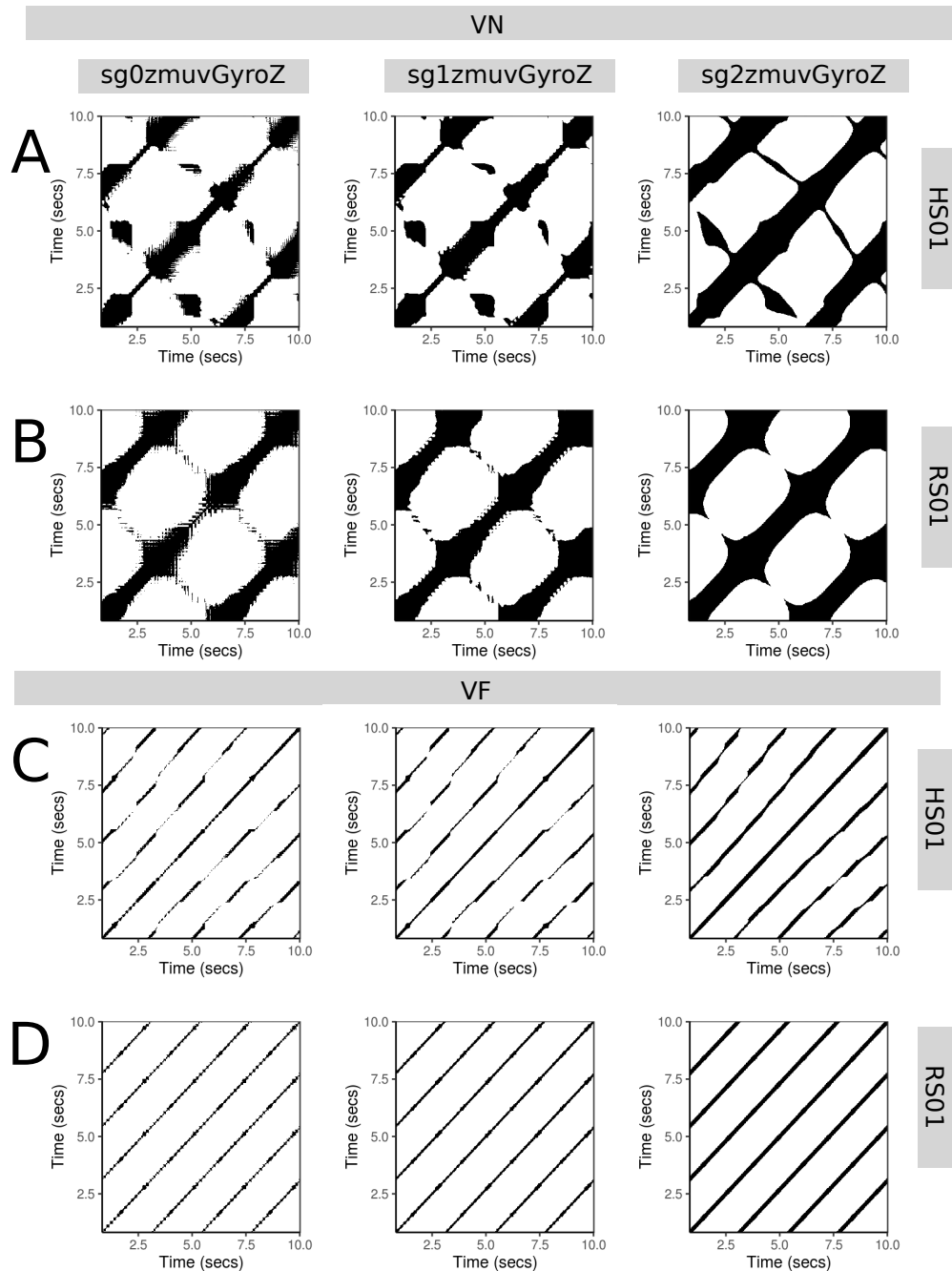


Fig. 6.7 RPs for vertical arm movements. Recurrence plots of participant *p01* for vertical movements in normal and faster velocity (VN, VF) with time series of raw-normalised (*sg0zmuvGyroZ*), normalised-smoothed 1 (*sg1zmuvGyroZ*) and normalised-smoothed 2 (*sg2zmuvGyroZ*), and sensors attached to the participant (HS01) and to the robot (RS01). Recurrence plots were computed with embedding parameters $\overline{m}_0 = 6$, $\overline{\tau}_0 = 8$ and recurrence threshold $\epsilon = 1$. R code to reproduce the figure is available at [\[link\]](#).

6.6 Recurrence Quantification Analysis

Considering the RPs for 20 participants performing four activities (HN, HF, VN and VF) with sensors attached to the human (HS01) and to the humanoid robot (RS01) and with the increase of smoothness of time series (sg0zmuvGyroZ, sg1zmuvGyroZ and sg2zmuvGyroZ), I hence compute four metrics of RQA metrics (REC, DET, RATIO and ENTR) with embedding parameters $\bar{m}_0 = 6$, $\bar{\tau}_0 = 8$ and recurrence threshold $\epsilon = 1$.

REC values

It can be seen in the box plots of Figs 6.8(A) that REC values, representing the % of black dots in the RPs, are more spread for HN and VN movements (higher interquartile range) than HF and VF movements (lower interquartile range) for HS01 sensor. In contrast, REC values for RS01 sensor present little variation (interquartile range of 0.01). With regard to the increase of smoothness of time series (sg0, sg1 and sg2), REC values present little variation as the smoothness is increasing for time series from HS01 (changes of mean values (rhombus)) while REC values are more affected with the smoothness for data from RS01 (see the incremental changes of mean values (rhombus)). See Figs F.19 and F.20 in Appendix F.5 for more details about individual REC values for each participant.

DET values

Figs 6.8(B) illustrate DET values, representing predictability and organisation of the RPs, which change very little (interquartile range is around 0.1) for type of movement, level of smoothness or type of sensor. See Figs F.21 and F.22 in Appendix F.5 for more details about individual DET values for each participant.

6.6 Recurrence Quantification Analysis

RATIO values

Figs 6.8(C) present RATIO values, representing dynamic transitions, for horizontal and vertical movements. It can be seen that RATIO values for HS01 sensor vary less for HN movements (interquartile range around 2) than HF movements (interquartile range around 5). It can also be noticed a decrease of variation in RATIO values as the smoothness of the time series is increasing (grey rhombus). See Figs F.23 and F.24 in Appendix F.5 for more details about individual RATIO values for each participant.

ENTR values

Fig. 6.8(D) show ENTR values, representing the complexity of the structure the time series, for both horizontal and vertical movements. ENTR values for HS01 sensor show more variation (interquartile range around 0.5) than ENTR values for RS01 sensor which appear to be more constant (interquartile range 0.1). It can also be said that the smoothness of time series affects each of the axis by an increase of mean values (see gray rhombos). See Figs F.25 and F.26 in Appendix F.5 for more details about individual ENTR values for each participant.

Quantifying Human-Humanoid Imitation Activities

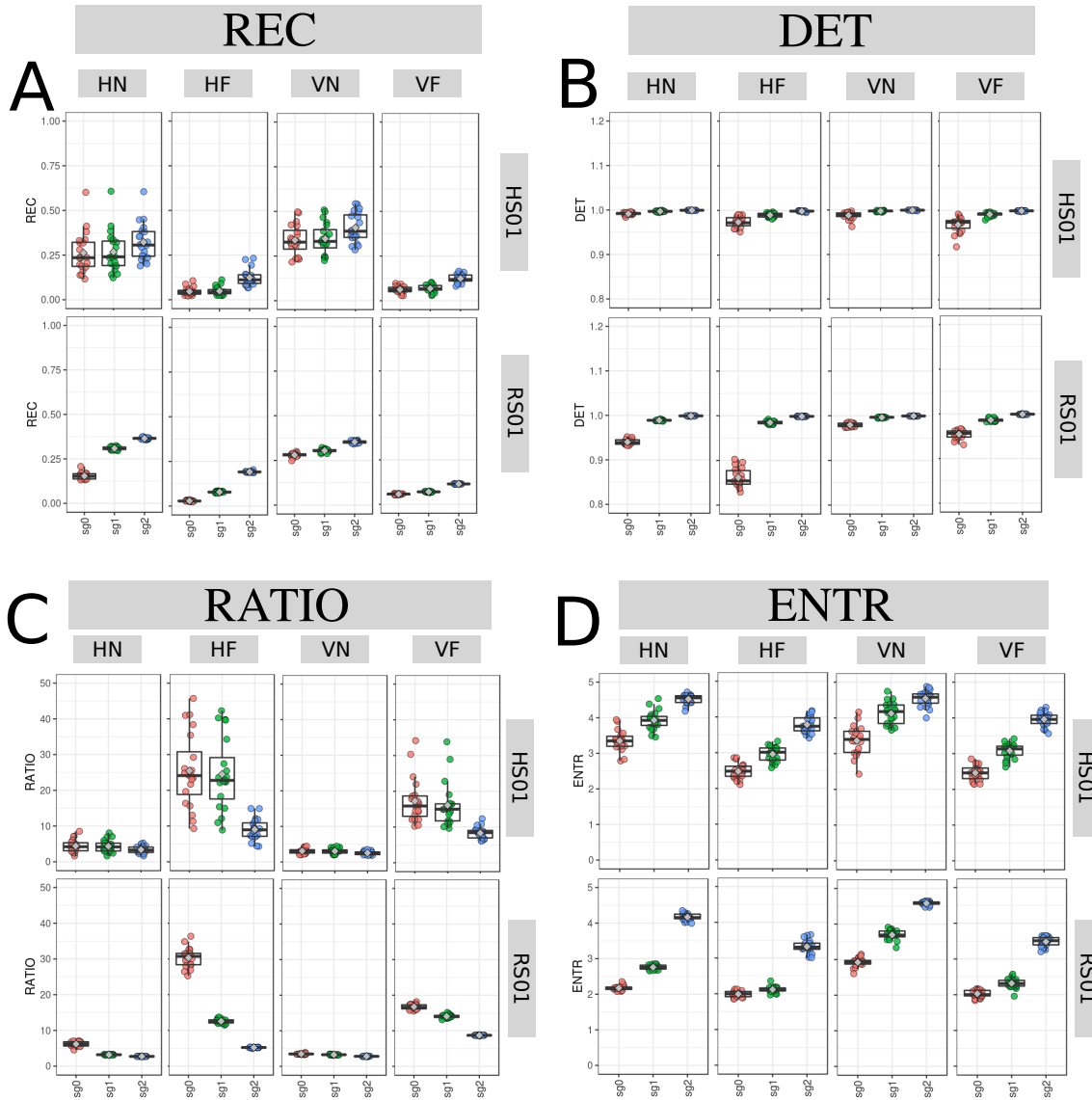


Fig. 6.8 **Box plots for RQA values.** Box plots of (A) REC, (B) DET, (C) RATIO, and (D) ENTR values for 20 participants performing HN, HF, VN and VF movements with sensors HS01, RS01 and three smoothed-normalised time series (sg0, sg1 and sg2). RQA values were computed with embedding parameters $\overline{m}_0 = 6$, $\overline{\tau}_0 = 8$ and recurrence threshold $\epsilon = 1$. R code to reproduce the figure is available at [DOI](#).

6.7 Weaknesses and strengths of RQA

Considering the Section 3.7.3 regarding the weaknesses and strengths of RQA, RQA metrics (i.e., REC, DET, RATIO and ENTR) are computed and plotted 3D surface plots using an unitary increase of pair embedding parameters ($0 > m \leq 10$, $0 > \tau \leq 10$) and a decimal increase of 0.1 for recurrence thresholds ($0.2 \geq \epsilon \leq 3$) (Fig. 6.9). Hence, Fig. 6.9(A) shows an increase for REC values, the percentage of black dots in the RP, as the recurrence threshold increases, while the variation for embedding parameters creates little decrease of REC values as the embedding dimensions increase and even slighter decrements of REC values for the increase of τ . For the 3D surface plots of DET values (Fig. 6.9(B)), representing predictability and organisation of the RPs, one can note a plateau for DET values near to 1 for embedding dimension parameters of less than 5 and recurrence threshold values of greater than 2 (red surface). It can also be observed that the increases of delay embedding made the DET values increase so as to make an cascade effect in the surface along with the increase of dimension embedding m . For RATIO values, representing dynamic transitions, Fig. 6.9 shows that the 3D surface plots present a plateau (blue surface) of RATIO values near to zero for recurrence thresholds greater than 1.0, while fluctuations are more evident for recurrence thresholds of less than 1.0, particularly it can also be noted an increase in the fluctuations of RATIO values as the embedding dimension is increasing. For ENTR values in Fig. 6.9(D), representing the complexity of the structures in time series, one can note that the increase of recurrence threshold is, not strictly proportional to the increase of ENTR values. It can also be observed in Fig. 6.9(D) that the increase of delay embeddings hardly affects the ENTR values for embedding dimensions of 1, while for higher values of embedding dimensions there is a decrease of ENTR values, and there is a decrease of ENTR values as delay dimension value is increasing.

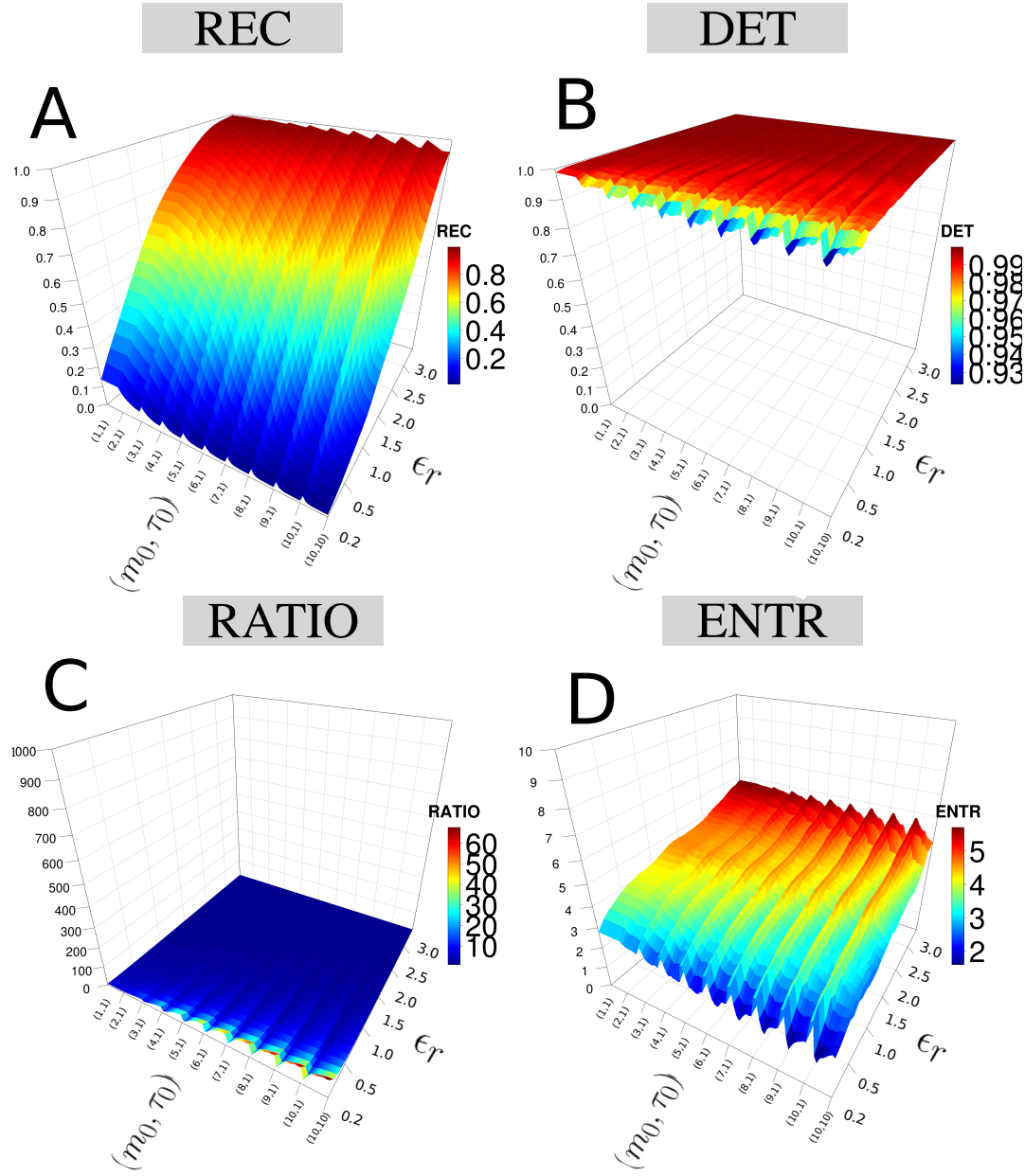


Fig. 6.9 3D surface plots for RQA metrics. 3D surface plots for (A) REC, (B) DET, (C) RATIO and (D) ENTR values with increasing pair of embedding parameters ($0 \leq m \leq 10$, $0 \leq \tau \leq 10$) and recurrence thresholds ($0.2 \leq \epsilon \leq 3$). RQA metrics are computed with the time series of participant p01 using HS01 sensor, HN activity, sg0zmuvGyroZ axis and 10 seconds for window length. R code to reproduce the figure is available at [DOI](#).

6.7.1 Sensors and activities

We also computed 3D surface plots of RQA metrics for different sensors and different activities (Figs. 6.10, 6.11), where it can generally be noted similar 3D surface plots patterns for RQA metrics as the ones in Fig. 6.9.

The 3D surface plots for REC values (Fig. 6.10(A)) show slightly differences with regard to vertical or horizontal activities however there are notable differences for normal and faster velocities, specially for the faster movements where the 3D surface plots shows a maximum REC value for embedding dimension values near to 1 and for recurrence thresholds near to 3. The 3D surface plots of DET values (Fig. 6.10(B)) and RATIO values (Fig. 6.10(C)) show slightly notable variations across the type of activities. For 3D surface plots of ENTR values it can be noted a slightly variation for surface plots of normal and faster velocities (Fig 6.10(D)).

As similar as Fig 6.10, the 3D surface plots patters for RS01 in Fig 6.11 show the differences between the activities performed at normal and faster velocities specially for REC and ENTR values (Fig 6.10(A, D)), while 3D surface plots for DET and RATIO values show slightly variations (Fig 6.10(B, C)).

6.7.2 Window size

Figs. 6.12 illustrate 3D surface plots for RQA metrics with four window lengths of 2-sec, 5-sec, 10-sec, and 15-sec. In general, it can be said that the increase of window length of the time series creates 3D surface plots patterns with better resolution.

Quantifying Human-Humanoid Imitation Activities

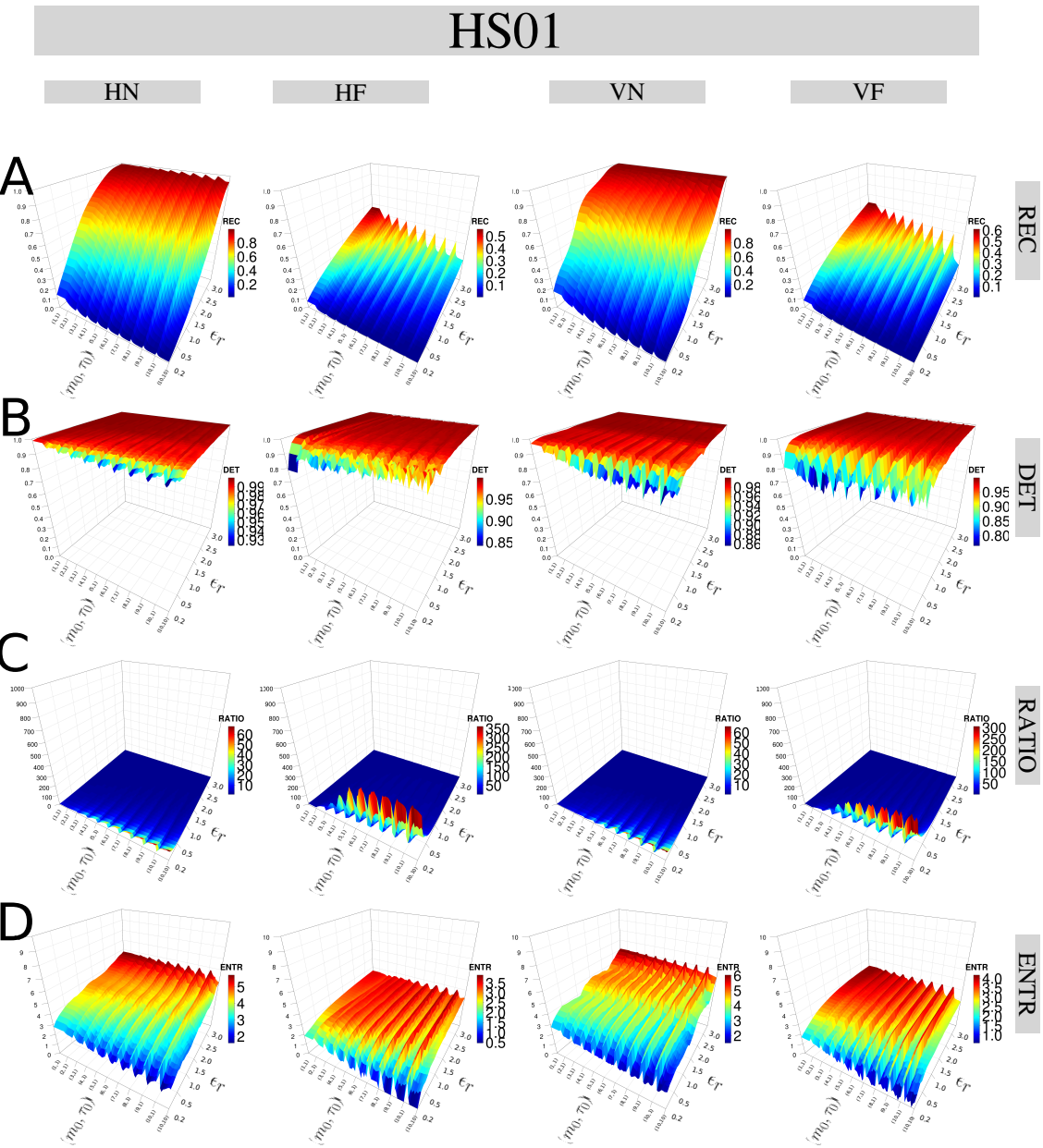


Fig. 6.10 **3D surface plots of RQA metrics for HS01 sensor.** 3D surface plots of RQA metrics ((A) REC, (B) DET, (C) RATIO, and (D) ENTR) with increasing embedding parameters and recurrence thresholds are for time series of participant p01 for sensors HS01, activities (HN, HF, VN and VF) and sg0zmuvGyroZ axis with 10 seconds window length. R code to reproduce the figure is available at [\[link\]](#).

6.7 Weaknesses and strengths of RQA

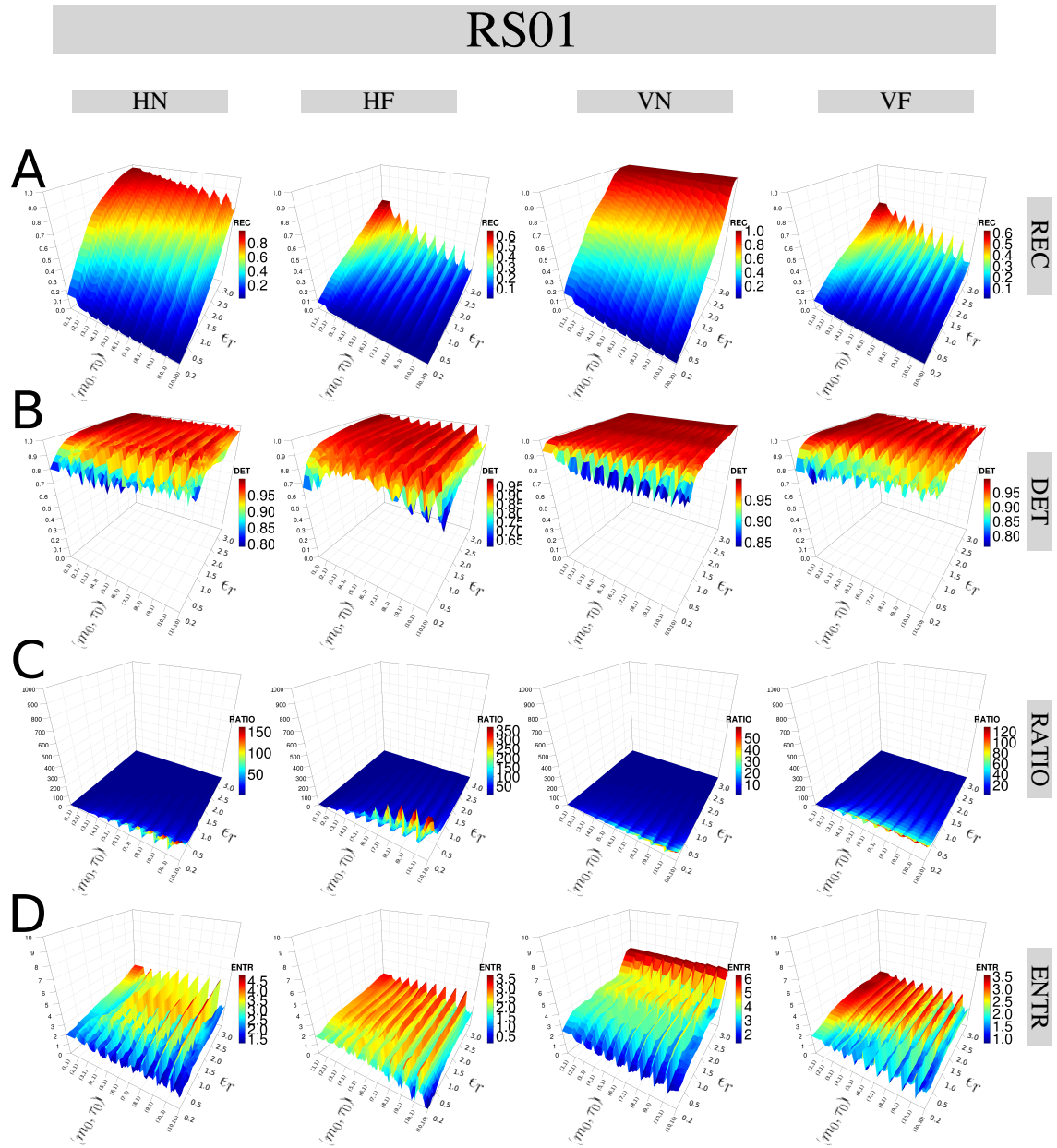


Fig. 6.11 **3D surface plots of RQA metrics for RS01 sensor.** 3D surface plots of RQA metrics ((A) REC, (B) DET, (C) RATIO and (D) ENTR) with increasing embedding parameters and recurrence thresholds are for time series of humanoid robot for sensors RS01, activities (HN, HF, VN and VF) and sg0zmuvGyroZ axis with 10 seconds window length. R code to reproduce the figure is available at [ϕ](#).

Quantifying Human-Humanoid Imitation Activities

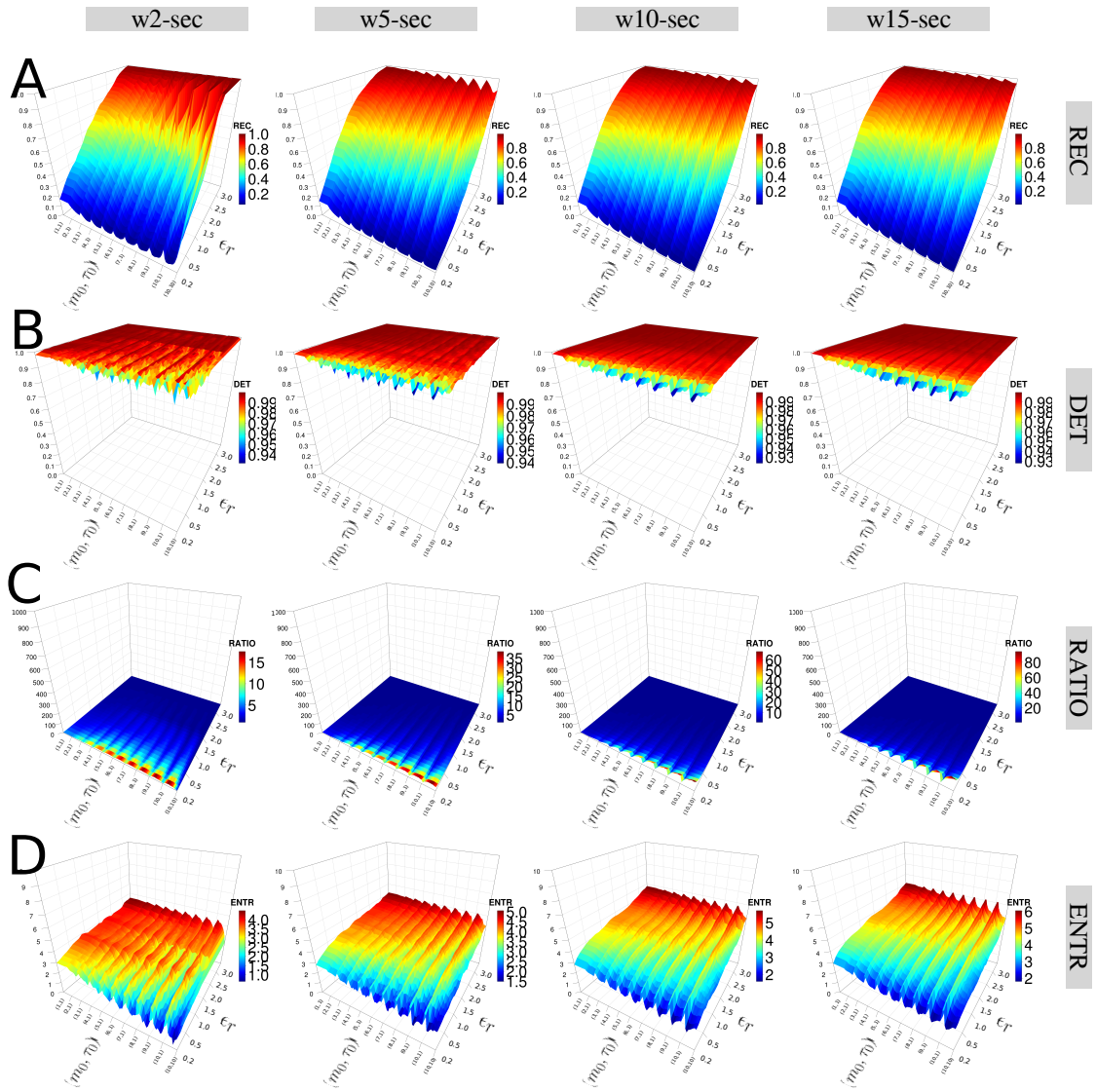


Fig. 6.12 **3D surface plots of RQAs metrics with four window lengths.** 3D surface plots of RQA metrics ((A) REC, (B) DET, (C) RATIO, and (D) ENTR) with increasing embedding parameters and recurrence thresholds for four window lengths (w2-sec, w5-sec, w10-sec and w15-sec). RQA metrics values are for time series of participant *p01* using HS01 sensor, HN activity and sg0zmuvGyroZ axis. R code to reproduce the figure is available at [\[4\]](#).

6.7.3 Smoothness

Figs 6.13 present 3D surface plots of the RQA metrics considering three levels of smoothness of the time series (sg0, sg1, sg2). It can then be noted that such smoothness have a direct effect on the smoothness of the 3D surface plots. Especially for dimension embeddings lower than 2 with in REC and ENTR values (Fig. 6.13(A, D)). The 3D surface plots of DET values are smoothed to a degree that the plateau (red surface) is increase, while RATIO values appear to be less affected to the level of smoothness (Fig. 6.13(C)).

6.7.4 Participants

Figs 6.14 illustrate 3D surface plots of RQA metrics for four participants. It can be noted that differences of the 3D surface plots across participants are more notable with REC (Fig. 6.14(A)) and ENTR values (Fig. 6.14(D)), while minor differences of 3D surface plots across participants are presented in DET (Fig. 6.14B)) and RATIO vales (Fig. 6.14(C)).

Quantifying Human-Humanoid Imitation Activities

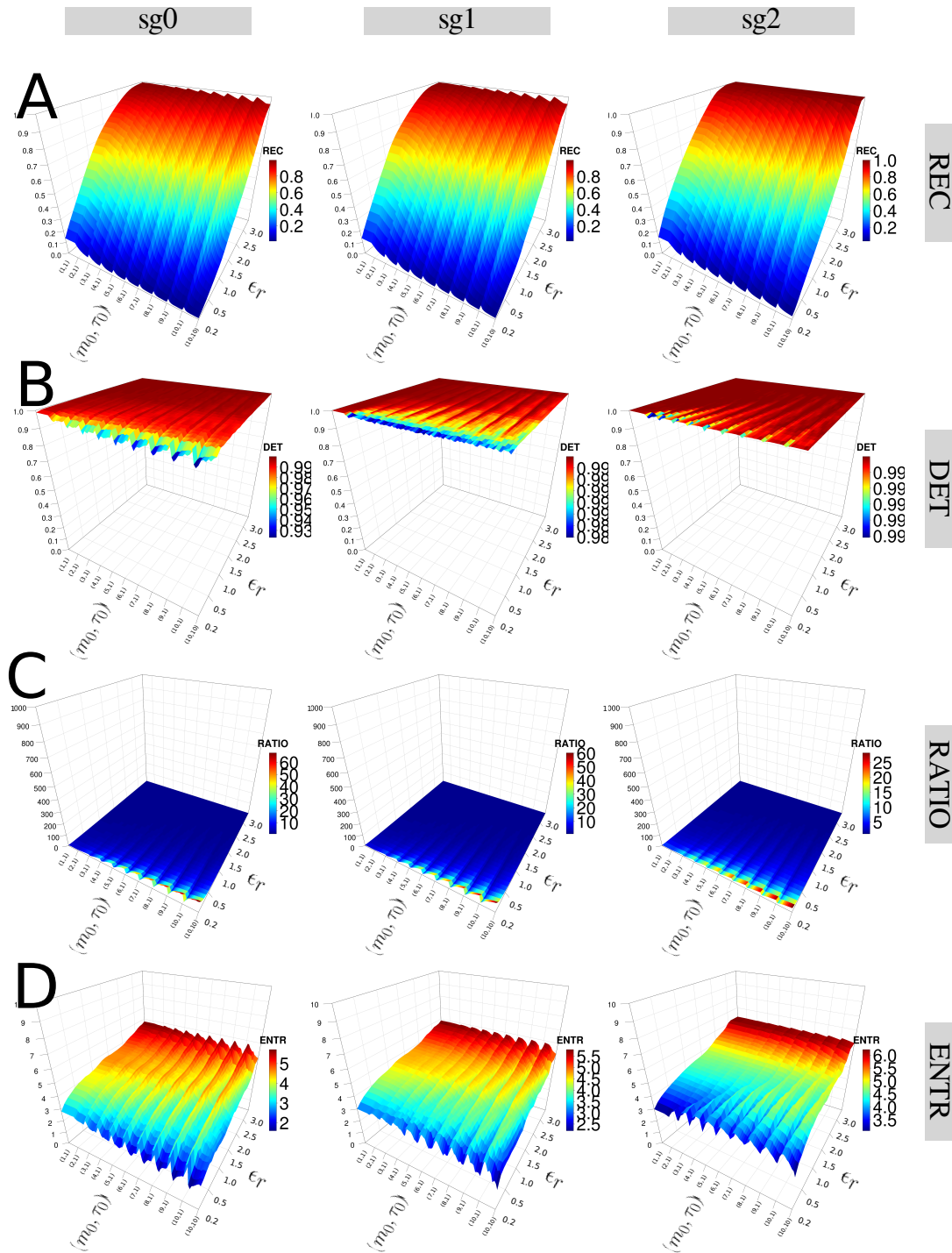


Fig. 6.13 3D surface plots of RQA metrics with three levels of smoothness. 3D surface plots of RQA metrics ((A) REC, (B) DET, (C) RATIO, and (D) ENTR) with increasing embedding parameters and recurrence thresholds for three levels of smoothness (sg0zmuvGyroZ, sg1zmuvGyroZ and sg1zmuvGyroZ). RQA metrics are computed from time series of participant *p01* using HS01 sensor, HN activity and 10 seconds window length. R code to reproduce the figure is available at [\[4\]](#).

6.7 Weaknesses and strengths of RQA

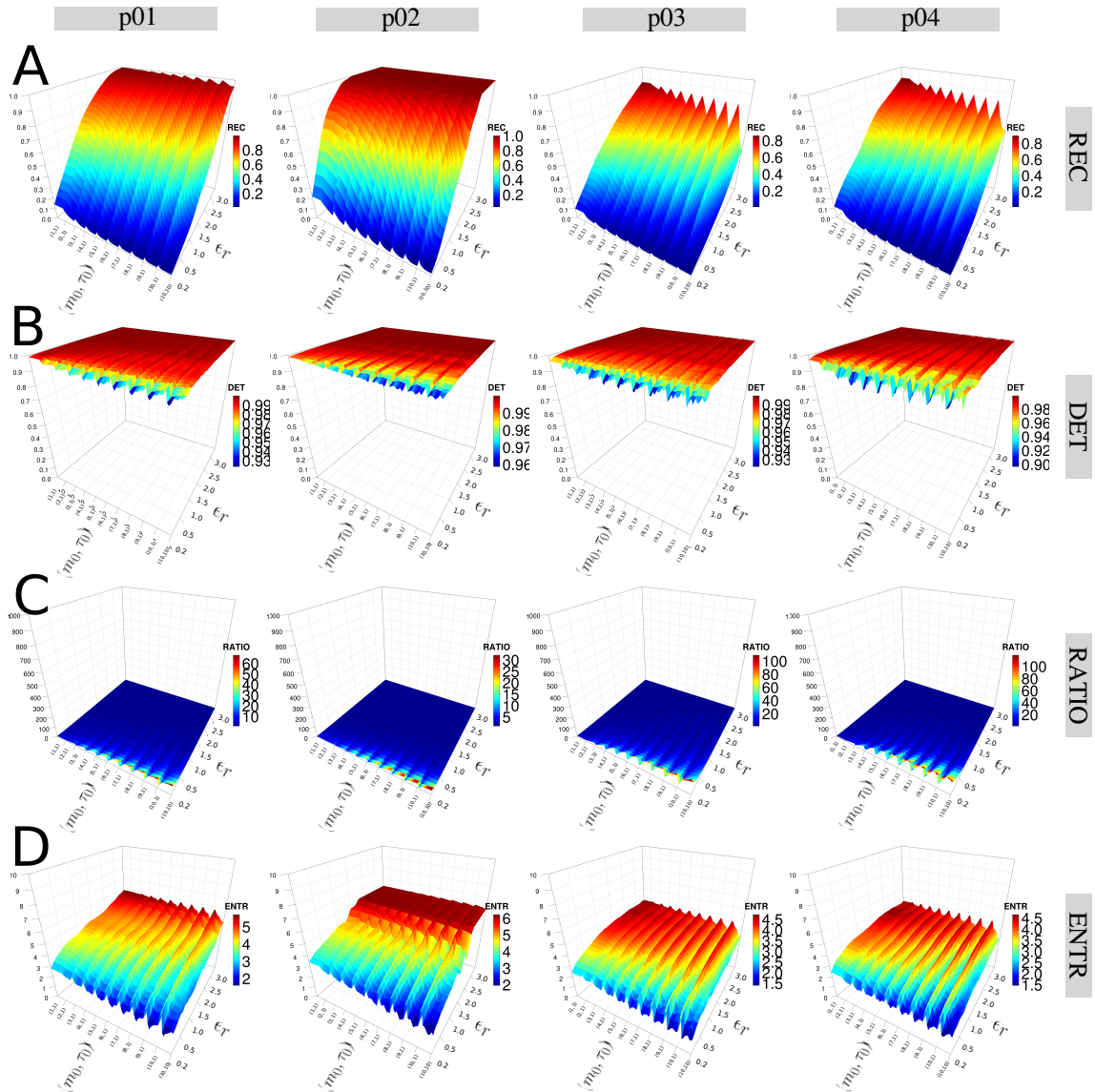


Fig. 6.14 **3D surface plots of RQA metrics with three participants.** 3D surface plots of RQA metrics ((A) REC, (B) DET, (C) RATIO, and (D) ENTR) for participants $p01$, $p02$, $p03$ and $p04$ with increasing embedding parameters and recurrence thresholds. RQA metrics values are for time series of HS01 sensor, HN activity and 10 seconds window length. R code to reproduce the figure is available at [🔗](#).

6.7.5 Final remarks

It can be noted that the changes of RQA metrics are evident with both the increase of embedding dimension parameters and the recurrence threshold for different structures, window size, levels of smoothness of the time series. For instance, RATIO values present a plateau (blue colour surface) which is independently to the source of time series, however there are peaks that change differently based on the source of time series. For DET values, 3D surface plots present a fluctuated surface (red colour) which slightly differs with the source of time series. With regards to REC values, 3D surface plots are affected by the velocity of movements. For example, surface plots for normal velocity presents an increase of REC values as recurrence threshold increases and keeping slightly uniform surface plot changes for the increase of embedding parameters. However for faster velocity arm movements, 3D surface plot fluctuations decrease as the embedding dimension increases and recurrence thresholds increases. Similarly as the results of human-image activities (see Section 5.7 in Chapter 5), 3D surface plots of ENTR values for human-humanoid interaction present changes to any of the types of time series which might be of help to understand the dynamics of movement variability in human-humanoid activities from different time series.